



Volume 115

2022

p-ISSN: 0209-3324

e-ISSN: 2450-1549

DOI: <https://DOI.org/10.20858/sjsutst.2022.115.15>

Journal homepage: <http://sjsutst.polsl.pl>



**Article citation information:**

Wheatley, G., Rubel, R.I. An autonomous braking control system for a 2017 Yamaha Grizzly 700. *Scientific Journal of Silesian University of Technology. Series Transport*. 2022, **115**, 211-226. ISSN: 0209-3324. DOI: <https://DOI.org/10.20858/sjsutst.2022.115.15>.

**Greg WHEATLEY<sup>1</sup>, Robiul Islam RUBEL<sup>2</sup>**

**AN AUTONOMOUS BRAKING CONTROL SYSTEM FOR A 2017 YAMAHA GRIZZLY 700**

**Summary.** Weed control is an important issue for environmental protection all around the world. Traditional hand weed control is laborious whereas chemical control is costly and a threat to the atmosphere. A chemical patch weed control system is an optimized system but lacks cheap technical equipment. This research outlines a design process and test of a braking system that can be applied during the designing of an autonomous braking system for a 2017 Yamaha Grizzly 700. The system is intended to be used as an autonomous weed chemical spraying. A bolt-on approach that did not require any manipulation of the stock, an internal braking system was followed to reduce the complexity and installation time of multiple systems. Three different types of autonomous braking system solutions were initially investigated, with the linear actuator solution being decided on through the assistance of a weighted decision matrix. The system was designed around a 30 kg hand force; however, a spare actuator of approximately 20 kg of force was repurposed and used instead. Finite element analysis concluded that all major components within the proposed system were suitable for a lifetime of at least 1,000,000 cycles with a mild steel yield stress failure criterion of 370 MPa. A stationary test for the system was conducted to determine the success of the system, which pushed the brake lever approximately 25% of its disengaged

<sup>1</sup> College of Science & Engineering, James Cook University, James Cook Dr, Douglas QLD 4814 Australia. Email: [greg.wheatley@jcu.edu.au](mailto:greg.wheatley@jcu.edu.au). ORCID: <https://orcid.org/0000-0001-9416-3908>

<sup>2</sup> Department of Mechanical Engineering, Bangladesh Army University of Science and Technology, Saidpur 5310, Bangladesh. Email: [rubel.ruet10@gmail.com](mailto:rubel.ruet10@gmail.com). ORCID: <https://orcid.org/0000-0001-8340-8877>

handlebar to lever length. The resulting system met the requirements of the expectation and could be used to apply the ATV's brakes autonomously while retracting the gear interlocking mechanism enough to change gears.

**Keywords:** weed control, hand and chemical control, autonomous braking system, FEA

## 1. INTRODUCTION

Australia is one of the largest agricultural industries [1][2] and weeds are one of the most serious threats to its environment [3][4][5]. Without proper control they can adversely affect crop health, leading to a decrease in farming productivity [3][4][5][6]. Purely through moisture competition between weed and crop, yields can be reduced by over 50% [5]. It is also estimated that the global damage from weeds costs 40 billion dollars per year [5]. To combat this, farmers spend long hours in the sun spraying crops with weed-killing agents. Weeding by hand is a traditional method of weed control; however, it is very costly [7]. In the United States alone, hand weeding costs \$9259/ha [8]. This is five to seven times more expensive than chemical control. Not only is this a safety risk, but replacing the necessity for human action could allow for labor to be spent more effectively in other areas [8].

More so, chemical control requires less manual labor for the same result. As observed, weed control using weed-killing agents appears to be the most effective solution [9]. Weed-killing agents may be distributed evenly across an agricultural area or sprayed in patches [9]. Although uniform spraying ensures most weeds are exposed to the agent, it can have detrimental effects on the crop. While very beneficial, weed-killing chemicals also have their limitations. The use of these chemicals can be detrimental to the crop, as well as the surrounding environment. Herbicides, chemicals designed to inhibit or kill the growth of plant pests, not only affect weeds but also mix with air, water, and soil [10]. There are two categories of herbicides: selective and non-selective. Selective herbicides only kill weeds without greatly damaging crops, whereas non-selective herbicides kill all plants in the application zone [10]. If a certain plot of land is continuously exposed to the same weed-killing chemical, the effectiveness drops. Pesticide concentration assessed in North America and Europe has shown substantial contamination in groundwater streams, both in agricultural and urban environments [11].

Spraying chemicals by the selective method to kill weeds and minimizing the chemical amount is thus a great challenge. Patch spraying can therefore be seen as an advantageous method of application. But identifying and applying chemicals in patches is also almost like traditional hand weed control [6]. Automatic identification and chemical spray are needed for the mechanized implementation of such an idea. However, for an autonomous scenario challenges arise in the complexity of computerized weed identification. Concerned with designing and building a weed-spraying system, a 2017 Yamaha Grizzly 700 all-terrain vehicle (ATV) is intended to modify [3][12]. The end goal for this system is autonomous control; however, the manual operation should still be possible while the automation process is running. The ATV will possess the ability to navigate autonomously with pathfinding and object detection.

Additionally, it will be equipped with onboard cameras and pattern recognition software to control weeds through target identification and patch spraying. As part of this project, the braking system of the selected vehicle is also required to modify adjusting to the targeted autonomous weed-spraying system. This part of the work is the design and validation of a mechanical braking system integrating electrical input control for the selected vehicle model.

The ideal design would allow overriding by an operator riding the ATV. Three different types of braking systems were considered for the proposal: a stepper motor, linear actuator, and solenoid driven system. The final decision on the most appropriate type of system for the design was assisted by a weighted decision matrix [13].

## 2. LITERATURE REVIEW

Patch weed control needs a system of identification and applying chemicals automatically to reduce manual labor [9][14]. In the market, a few types of patch weed control machines are available; however, price and size have made it acceptable for only huge farmland applications and not for day-to-day applications for small to mid-range applications. To make something for small to mid-range applications, we were looking for low-cost, easily driveable, and customizable vehicles. Since weeds grow in the fields, the type of the selected vehicle should be an off-road vehicle. A four-wheeler Yamaha Grizzly 700 ATV [12] was found suitable for the intended weed-spraying system to modify or customize on our own. We have concise our focus on the brake customization for the selected vehicle in this work in weed spraying application.

Yamaha Grizzly 700 ATV [12] has a stock braking system that features dual front and rear hydraulic disc brake systems. The right-hand brake lever is connected to the front wheel braking system, while the left-hand brake lever is connected to the rear wheel braking system. There is also an additional foot brake on the right-hand side of the vehicle with a direct-acting cable link to the left-hand brake lever. In the case of this bike's system, the master cylinder reservoir is disconnected from the hydraulic line by a single spring and piston component. Any excess force is transmitted directly into the hydraulic line. At the other end of the hydraulic line is a slave cylinder at each wheel (only considering one brake line). Since the slave cylinder piston's area is larger than the master cylinder piston's area, it travels less; however, exerting a larger force. This force is applied to the brake disc through the caliper's two brake pads. The first brake pad clamps down on the brake disc due to the pressure in the hydraulic line. Since the caliper housing is allowed to translate away from the first pad that is in contact with the disc, excess force results in the second pad clamping on the opposite side of the brake disc. A force beyond this is evenly distributed between the two brake pads, ensuring even wear.

## 3. METHODOLOGY

### 3.1. Handgrip strength

To determine an appropriate force to design the braking control system around, research was conducted into typical handgrip strengths for males and females in different age categories. Table 1 shows that the average right- and left-hand grip strengths for men between the ages of 20 and 59 are 46.5 and 45 kg, respectively [15]. It also shows that the average right- and left-hand grip strengths for women between the ages of 20 and 59 are 29.5 and 27.75 kg, respectively. The highest pressure that the braking system reached is 14 bar or 1.4 MPa according to a braking profile for a motorbike braking while traveling above 100 km/h.

Tab. 1

Mean and standard deviation and hand grip strength in kilograms, for men and women, presented in ascending age groups [15]

Men				Women			
Age	Right	Left	BMI	Age	Right	Left	BMI
20 to 29	47(9.5)	45(8.8)	26.4(5.1)	20 to 29	30(7)	28(6.1)	25.1(5.8)
30 to 39	47(9.7)	47(9.8)	28.3(5.2)	30 to 39	31(6.4)	29(6)	27.3(6.8)
40 to 49	47(9.5)	45(9.3)	28.4(4.6)	40 to 49	29(5.7)	28(5.7)	27.7(7.7)
50 to 59	45(8.4)	43(8.3)	28.7(4.3)	50 to 59	28(6.3)	26(5.7)	29.1(6.4)
60 to 69	40(8.3)	38(8)	28.6(4.4)	60 to 69	24(5.3)	23(5)	28.1(5.1)
70+	33(7.8)	32(7.5)	27.2(3.9)	70+	20(5.8)	19(5.5)	27(4.7)

Examining the data in Table 1, a handgrip strength value of 30 kg (approx. 300 N) was initially chosen to design around. For justification, initial calculations using the chosen value and the fundamental equations were conducted. Fundamental terms like the deceleration rate, stopping distance, and force a driver can apply to the master cylinder are determined by the relation  $DR = \mu g$ ,  $SD = V_{max}^2/2DR$ , and  $F_{mc} = F_{driv} \times 4$ . The pressure developed by  $F_{mc}$  in the hydraulic line is  $P_{line} = F_{mc}/A_{mc}$ , and the force on the caliper is  $F_{cal} = P_{line} \times A_{cal}$  where the force on the rotor is  $F_{rot} = F_{cal} \times 2$  [16]. Thus, the total frictional force will be created as  $F_{fric} = F_{rot} \times \mu$ , and the torque on the rotor will be  $\tau_{rot} = F_{fric} \times r_{rot}$ . The final force acting on one tire will be  $F_{tyre} = r_{rot}/r_{tyre}$  [17].

Originally, a 700 N, 11.5 mm/s linear actuator was selected for the design. This was changed to the 200 N, 35 mm/s actuator, which did not suit its purpose for the bike's gearing system. This actuator was approximately three times as fast, and the repurposing saved from having to buy another actuator. The downside was the reduction in output force. While the repurposed actuator did not output 30 kg of hand force, this value was deemed over conservative since it was chosen from maximum hand forces and was not required for an appropriate level of brake actuation.

Tab. 2

Estimated values of the necessary parameters

Parameters	Values	Parameters	Values
$A_{mc}$	$5.067 \times 10^{-4} \text{ m}^2$	$F_{mc}$	1177.2 N
$F_{driv}$	294.3 N	$P_{line}$	2.323 MPa
$W_{bike}$	314 kg	$F_{cal}$	$2.323 \times 10^{+6} \times A_{cal}$

Since  $A_{cal}$  could only be obtained by disassembling the physical caliper on the ATV, and this was only a preliminary calculation, it had been temporarily assumed that  $A_{cal}$  was approximately two times greater than  $A_{mc}$ . The corresponding  $F_{cal}$  is 2.35 kN. The pressure experienced in the designed system was predicted to be approximately 2.3 MPa, which demonstrated that there would be enough braking force applied.

### 3.2. Decision about the type of brake

To assist in the decision-making process for the type of braking control system to use, a weighted decision matrix [13] table was constructed with the results shown in Table 3.

The three systems were compared against each other on a relative scale out of 10. For example, stepper motors and solenoids found online were both upwards of \$200. The linear actuator found, however, was only around \$80. Approximate relative values of 6 for the stepper motor and solenoid and 10 for the linear actuator were chosen for the matrix in the cost of system row [18]. The weighting was determined by the importance of each criterion to ensure that critical factors were assigned a higher score. From the decision matrix shown in Table 3, it was clear that the linear actuator braking system design was by far the most appropriate choice.

Tab. 3

Weighted decision matrix for braking system type

Criteria	Weighting (/10)	Stepper Motor	Linear Actuator	Solenoid
Reliability	10	9	9	9
Speed	7	8	10	10
Suitability	6	7	7	4
Cost of System	5	6	10	6
Simplicity	4	9	9	9
Total		254	288	250

### 3.3. Selected system for design

The chosen design consisted of the following major components:

- A Barkbusters handlebar insert as a frame for the actuator, \$90.00 from Motosport Townsville.
- A 200 N, 35 mm/s, 12 V, 50 mm stroke linear actuator, \$84.65 from Motion Dynamics.
- Custom machined mounting plates to fix the actuator to the Barkbusters frame.

The linear actuator was intended to be fixed onto the Barkbusters frame. Originally, the actuator was designed with a 300 lb strong wire set up to pull the brakes as the actuator retracts. Since the team required a more robust and reliable solution, this design was reversed such that the actuator would push the brakes with a custom front plate for this purpose. This proposed system costs approximately \$200.

The success of this design is to be determined through testing of the finished quadbike braking system. Time and quadbike status constraints limited the final test to be stationary, with success visually determined by the degree of braking achieved and the clearance of the gearing interlock mechanism for shifting gears while braking. Prototyping of the braking system design was considered; however, due to the simplicity and robustness of the solution, this was not required. The linear actuator load strength rating was validated visually by ensuring it could activate the brake lever to a satisfactory degree before it was trusted for autonomous use. A braking test at multiple speeds was initially planned; however, due to the state of the vehicle during testing, only a stationary test could be conducted. Finally, finite element analysis (FEA) was performed on both the Barkbusters frame, as well as the custom mounting plates and front interfacing plates, to determine the stress profiles under standard operation, as well as the simulated hand force, which would lead to failure with fatigue testing. This was conducted using Solidworks for the CAD modeling and the Static Structural FEA package within ANSYS for stress analysis.

### 3.4. CAD model development

To determine the geometry of the custom parts required for the braking system, mock models for the linear actuator, handlebar, and the Barkbusters frame were created in Solidworks. Most of the linear actuator's dimensions were provided by the manufacturer; however, some were omitted. Fortunately, the critical dimensions were known such that an accurate enough model could be constructed. A set of Kincome digital Vernier calipers were used to determine the exact dimensions of the Barkbusters frame and handlebar. Since the brake lever itself was a complex geometry that could not be replicated without 3D scanning, a rough estimation was used for the mock model in Solidworks. Estimations of the distance between the handlebar and brake lever were recorded with the calipers and replicated in the CAD assembly. Finally, the custom plates used for mounting the actuator to the Barkbusters frame, and the front plate, which was used to directly push the lever, were designed. The custom parts required, shown in blue in Figure 1, were manufactured at the James Cook University mechanical workshop.

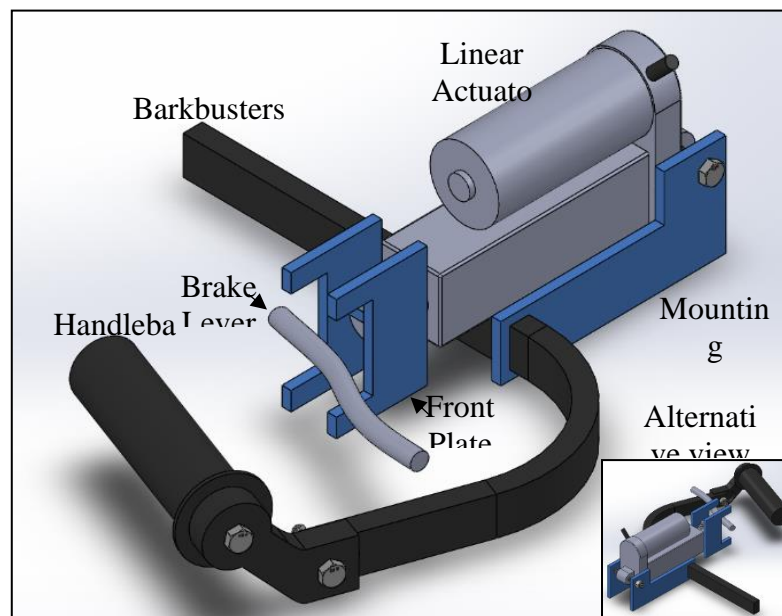


Fig. 1. Solidworks design

## 4. RESULTS AND DISCUSSIONS

### 4.1. Finite element analysis of the system

Finite element analysis was performed on three parts within the newly designed autonomous braking system: the mounting plate, the front plate assembly, and the Barkbusters frame. Each model was analyzed for von Mises stress, with the failure criterion specified at 370 MPa, the approximate yielding point for mild steel [19]. Fatigue analysis using the Goodman method was also performed with a lifetime of 1,000,000 zero-based cycles.

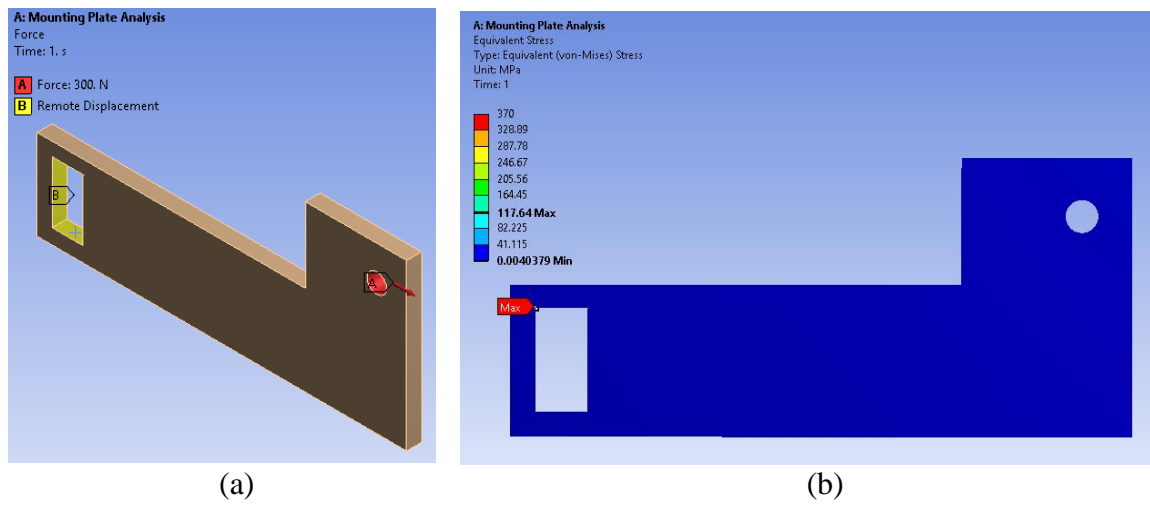


Fig. 2. (a) Mounting plate FEA setup, (b) Mounting plate FEA von Mises stress

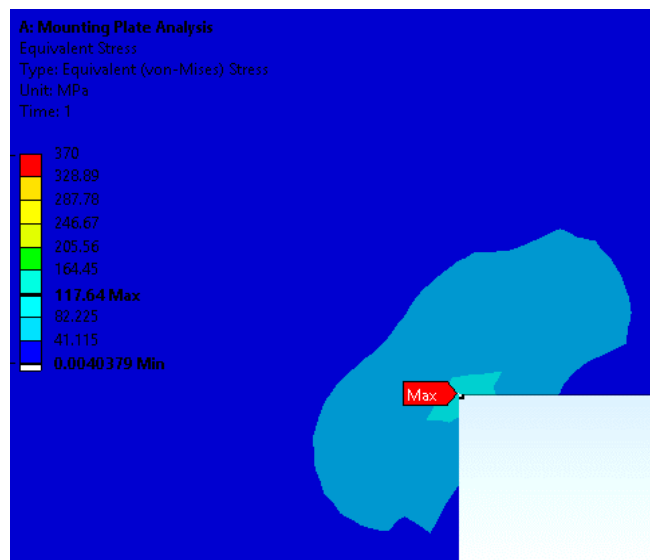


Fig. 3. Mounting plate FEA von Mises stress (close-up)

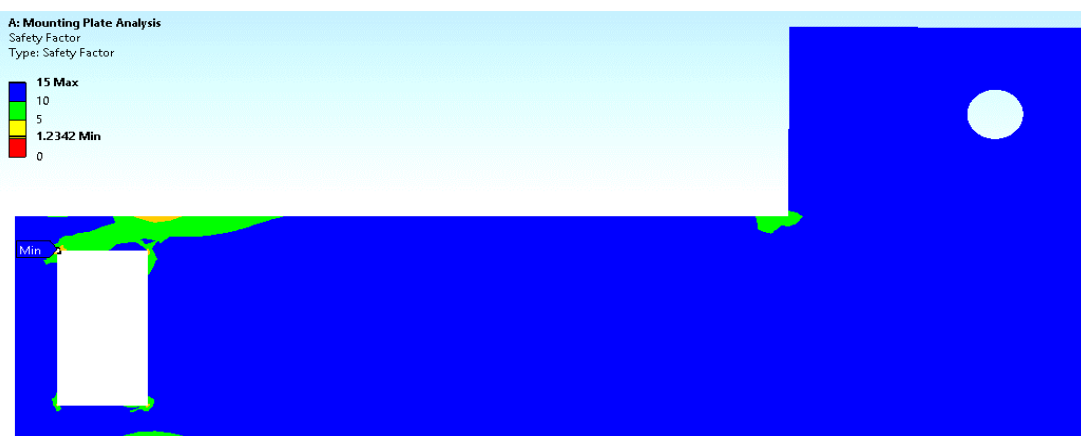


Fig. 4. Mounting plate FEA Safety Factor



Fig. 5. Mounting plate FEA safety factor (close-up)

Originally, the system was designed around a 300 N actuation force. Instead of reducing the force used within the FEA to 200 N to match the actuator's maximum output, a decision was made to maintain the system's design based on the 300 N force. This conservative approach ensured that the parts to be manufactured were without a doubt strong enough to last well beyond their required lifetime, especially necessary in a critical autonomous braking system. Figures 2-5 show that the mounting plate design was appropriate to ensure a full life. The system was set up with restrictive remote displacement support at the faces within the slot for the Barkbusters frame, and a 300 N force was applied at the cylindrical face acting to the right. The resulting maximum von Mises stress was found to be approximately one-third of the yielding stress, and the fatigue analysis showed that no sections would fail before the end of their lifetime. The safety factor is shown as 1.23; however, this is only in a small region of stress concentration. The safety factor increases above 10 slightly beyond this region, so at worst, a small crack would form. To reduce concerns even further, the Barkbusters frame has rounded edges, which would provide some relief to the stress concentration.

Figure 6 shows that the front plate design for pushing the brake lever is suitable and ensures a full lifetime. The system setup included a 300 N force acting on the two front surfaces of the assembly and a remote displacement to restrict movement and rotation at the cylindrical surface. As seen in Figure 6(b), the front plate did not experience any significant stress, further validated by the safety factor shown in Figure 7(a). This shows that this manufactured part should easily exceed its required lifetime.

Figures 7(b)-10 show that the Barkbusters handlebar insert frame should also exceed its required lifetime. The system was set up with restrictive remote displacement support at the furthest cylindrical face, and two 150 N forces spaced 45 mm apart (the spacing of the mounting plates). Figure 8 shows that the system only experiences approximately one-third of the yielding stress of mild steel. When fatigue is investigated, the safety factor was found to be 1.37 (Figure 10). This is not actually a concern for two reasons. First, the fatigue analysis is conducted over 1,000,000 cycles. The actual cycles within the part's realistic lifetime would be severely less than this. This analysis shows that even with such an extended lifetime, the part still does not fail (despite it being close). The second reason is that the actual material of the Barkbusters frame is unknown. This analysis assumes a worst-case material, which is mild steel. In reality, it is likely that the material used is much stronger and resists bending even further since it was designed for impact protection. Furthermore, it is also important to consider that not all dimensions of this mock model are accurate.



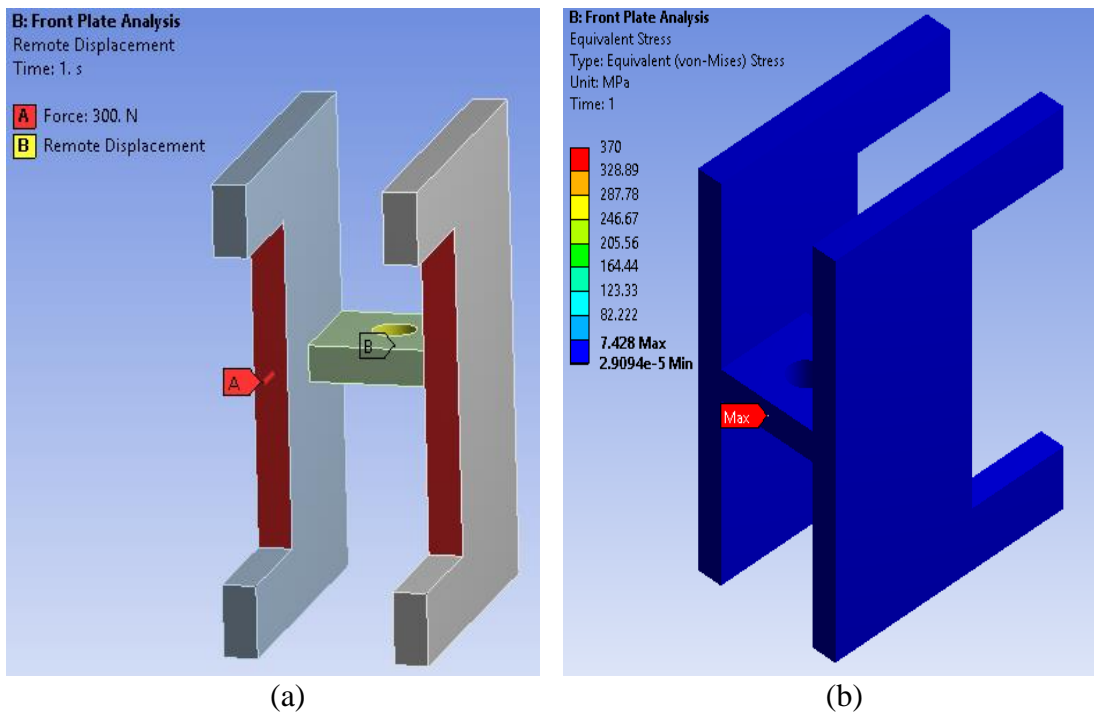


Fig. 6. (a) Front plate FEA setup, (b) Front plate FEA von Mises stress

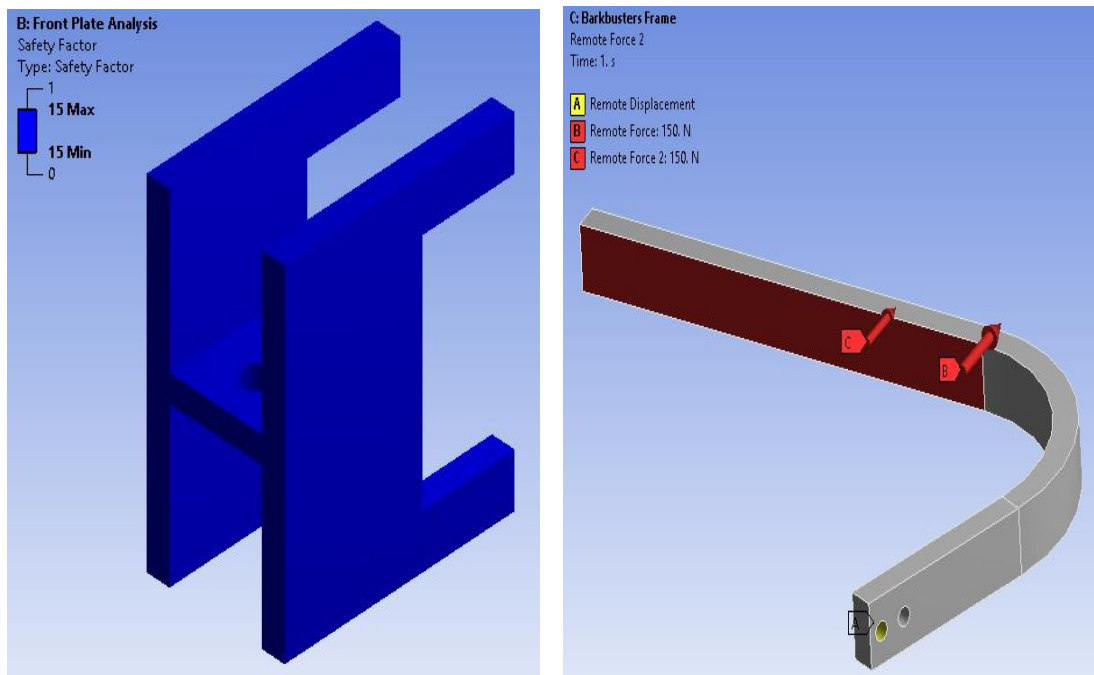


Fig. 7. (a) Front plate FEA safety factor, (b) Barkbusters frame FEA setup

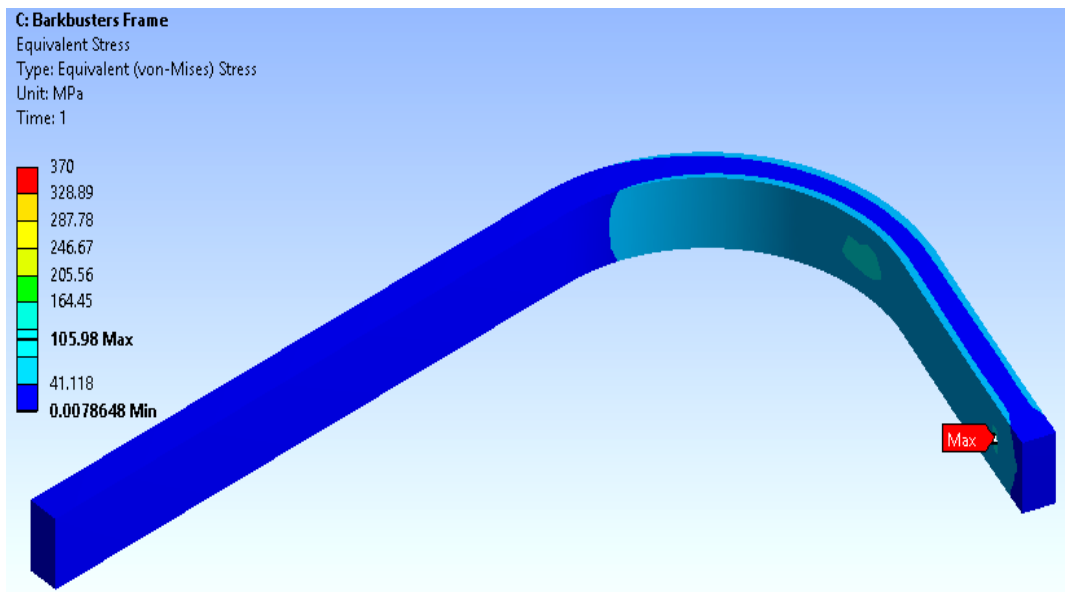


Fig. 8. Barkbusters frame FEA von Mises stress

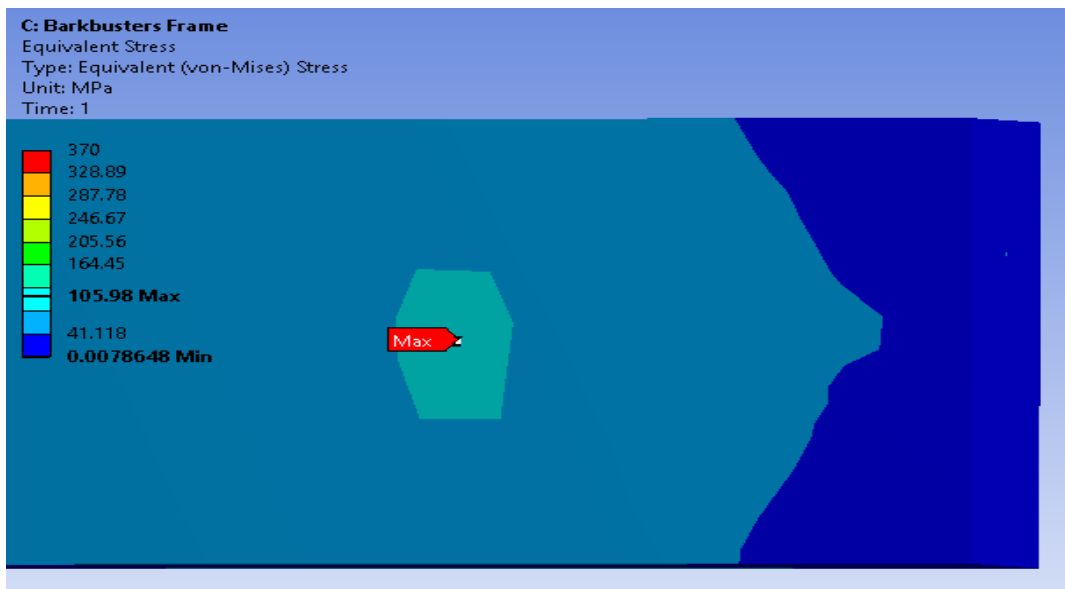


Fig. 9. Barkbusters frame FEA von Mises stress (close-up)

The critical dimensions such as the diameter and location of the holes and height and thickness of the bar were measured with the Vernier calipers; however, the exact length of the bar sections and curve profile were not known, so they were approximated. The actual curved profile of the Barkbusters frame was likely better designed to resist failure due to bending. Additionally, as stated earlier, the actuation force was one-third lower at 200 N. For all the reasons stated above, it was concluded that the Barkbusters frame was suitable for use in the autonomous braking system.

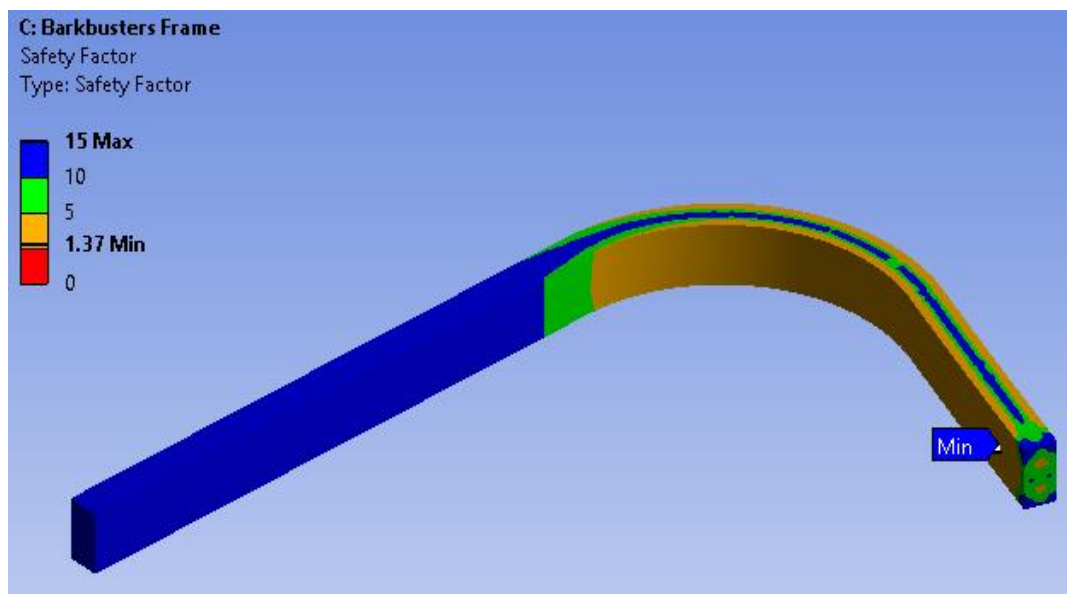


Fig. 10. Barkbusters frame FEA safety factor

## 4.2. System testing

Once the parts were deemed safe for use, the system was ready for assembly and testing. The system was positioned on the frame such that actuation occurred as far away from the pivot point to increase the lever arm and reduce the force requirement. The mounting plates were then fixed in position with a hose clamp on either side. An H-bridge circuit with a forward and reverse button was coded and set up [20]. The setup of the system is shown in Figure 10. As stated earlier, the test was conducted on a stationary quadbike, with success determined visually by the degree of braking achieved, including the clearance of the interlocking mechanism on the gearing.

Once all the parts had arrived and were ready for assembly, a complication was discovered with the design of the ATV's handlebars. Upon removing the rubber grips, it was evident that despite the Barkbusters website providing the specific part to fit this make and model, the handlebars were not completely hollow as seen in Figure 11(a). Approximately 7 mm deep, it appeared a metal "plug" had been hammered in and welded. The Barkbusters handlebar inserts required a hollow handlebar for attachment since this design used an internal collet to grip the inside of the handlebar. A simple acoustic test was performed to determine the length of the inner metal and found that it extended beyond the requirement of the collet. Upon consultation with relevant experts, a decision was made to drill into the metal, stepping up to 14 mm since this was approximately 0.5 mm larger than the collet diameter. An alternative solution of drilling and tapping the hole for the M8 bolt was considered. This, however, was considered more difficult since the hole would have to be drilled almost perfectly straight for the tapping to work.

To drill the metal in the handlebar out to 14 mm, it was found that multiple step-ups were required. What was not known was how many millimeters each step should be. To start conservatively, a step size of 3 mm was chosen. The depth of the cut required was marked on the handlebar, shown in Figure 11(b). Starting at 3 mm, half of the cut was made. Copious amounts of cutting fluid were used to reduce the difficulty of the cut, as well as increase the drill bits' lifespans. The drill was retracted every 20 to 30 seconds and compressed air was

sprayed into the cut to clear metal fragments. A decision was then made to split the drilling depth into two stages of cuts since progress increasingly slowed down as metal shavings struggled to travel up the bit to exit the hole. A jump of 4 mm from a 6 mm to 10 mm diameter was attempted; however, this was reverted to 8 mm before the 10 mm cut since the drilling jobber started to smoke and struggle. Figure 11(c) shows the progression of these cuts. Finally, 12, 13, and 14 mm cuts were made. This allowed the Barkbusters frame to be successfully inserted into the handlebar, where it was able to be secured using the collet.

As evident in Figures 12-14, the result of the braking system test was a success. The system was shown to activate the brakes to an acceptable degree, validated by the clearance of the gearing interlock mechanism. This allowed the gears to be changed once the brakes are applied. Overlaying the green lines shown in Figures 12-14 and measuring the percentage difference showed that the approximate lever movement was 25% of the disengaged distance from the handlebar. Despite the success of the system, the gear interlocking mechanism would be better off with more clearance. Future recommendations on this topic are discussed in a later section.

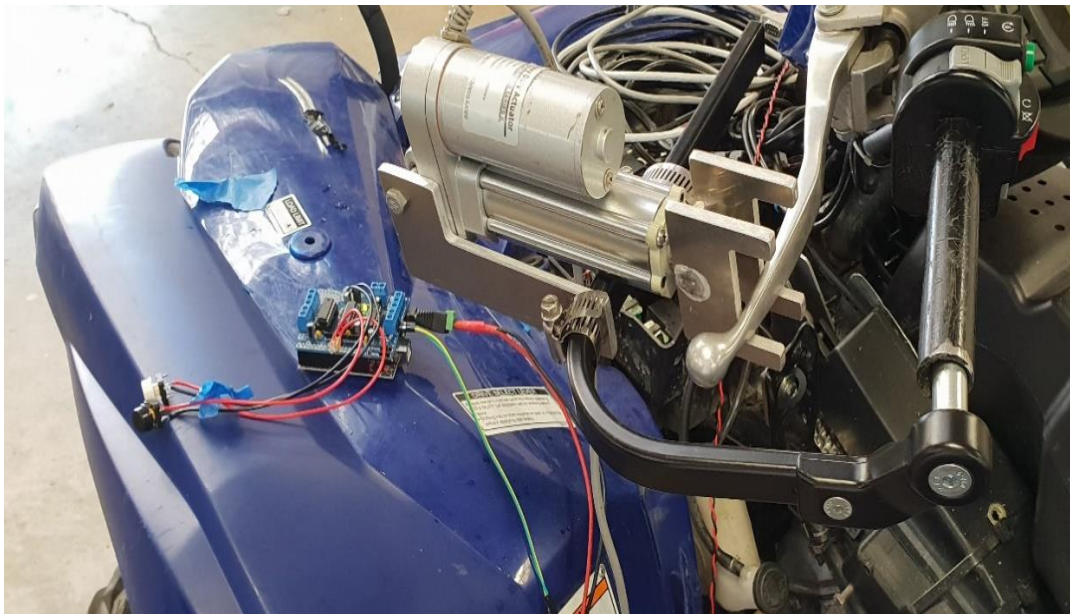


Fig. 10. Full assembly during testing

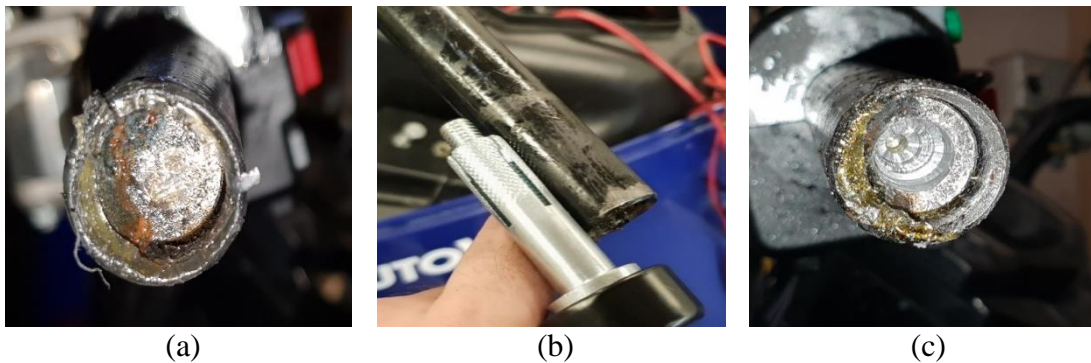


Fig. 11. (a) Metal "plug" discovered in handlebar, (b) Marking for depth of drilling cut, (c) Drilling step-up progress



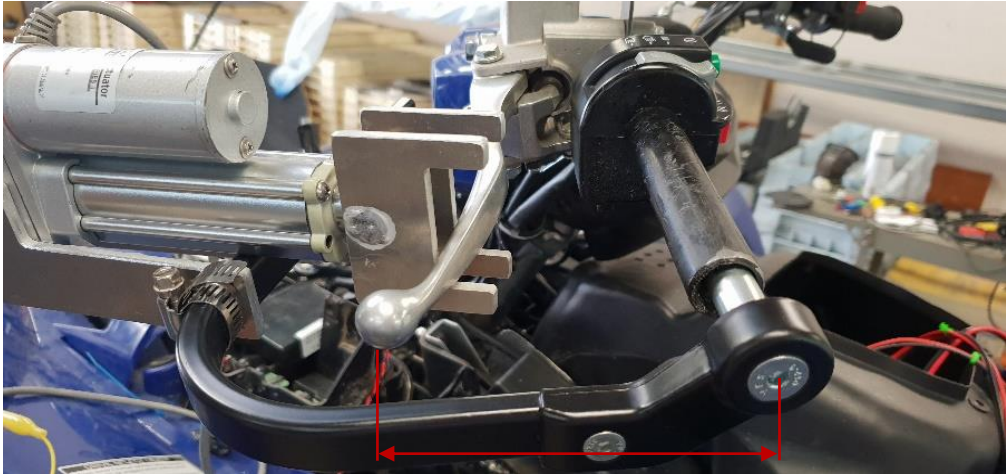


Fig. 12. Braking system test-system disengaged

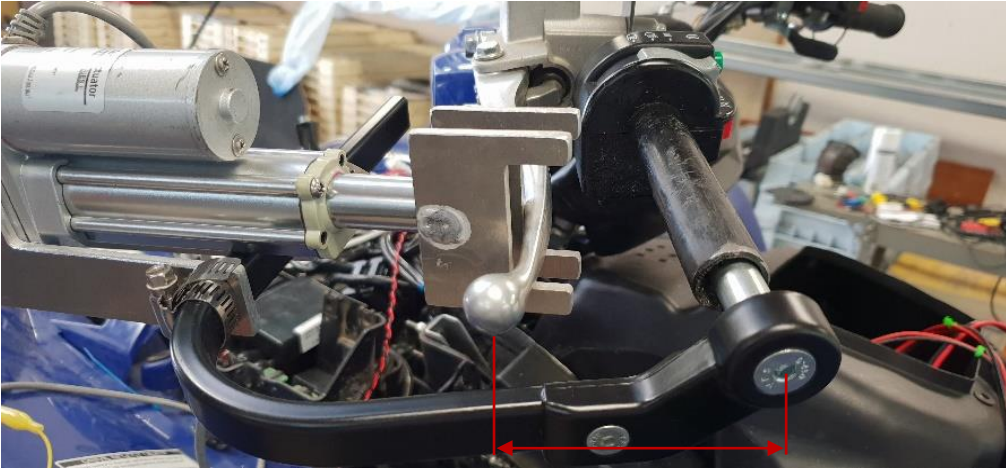
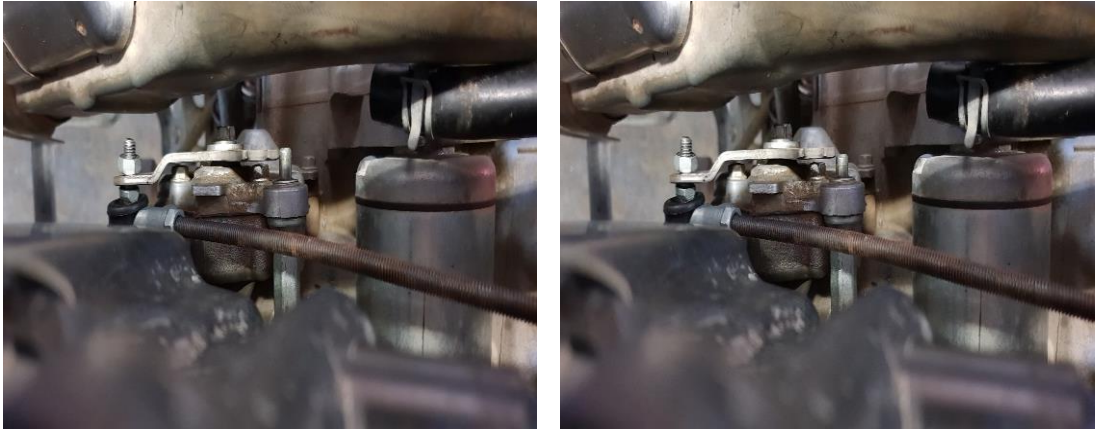


Fig. 13. Braking system test-system engaged



(a) (b)  
Fig. 14. (a) Gear interlock mechanism-system disengaged,  
(b) Braking system test-system engaged

#### 4. CONCLUSION

This work has successfully designed and tested the autonomous braking control system for a 2017 Yamaha Grizzly 700. The resulting designed system is capable of satisfying the requirements needed in the field for weed control. In its current state, the system could apply and release the ATV's brakes through an external H-bridge circuit with a forward and reverse button. The gear interlocking mechanism retracts enough for gear switching; however, it is a small clearance. Finite element analysis conducted through ANSYS' Static Structural package confirmed the reliability of the system well beyond its expected lifespan. The mechanical components within the system were conservatively designed, ensuring that a system as critical as the braking on an autonomous vehicle would not fail unexpectedly and could be trusted. The mechanical components of the system are fully designed, although further refinements may be beneficial depending on the future vision and direction of the team. The total weight of the components in the braking system was negligible compared to the original vehicle weight, and thus, no issue of balancing or counterweighting. Simple construction is also removable in any case if needed. Additionally, the modification is cost-effective as the total cost required for the whole setup and integration cost lies only \$1000 much lower than any presently available commercial vehicle. The cost of the components was a reasonably weighted factor in the decision of the system type for design. The total price for the chosen system is expected to be approximately \$200 for a commercially anticipated setup. The 2017 Yamaha Grizzly 700 did not lose its normal functions and usability even after the setup of the braking system for weed control, which may be regarded as a dual benefit.

#### 5. RECOMMENDATIONS

Since the clearance of the gear interlocking mechanism is small, a few future changes to the system would be beneficial. First, the actuator could be upgraded to ensure a greater braking action. Generally speaking, a more powerful actuator results in a slower speed unless a significant price increase is met. This could be countered by fixing the actuator closer to the pivot point of the brake lever, resulting in a lower travel requirement and larger force requirement. Testing would be required to ensure that the travel force/speed trade-off would balance positively for the system. Alternatively, as suggested by an expert, a cleaner wiring solution for the circuit may be beneficial. The current electrical circuit consists of daisy-chaining solutions using old spare wires. With fewer resistances and losses from exposed and inefficient wiring, the voltage provided would be higher, and hence, the clearance of the mechanism would increase. Finally, if necessary, two actuators could be used for the single brake lever. This would also be beneficial as a backup if one actuator malfunctions. With the purchase of another identical actuator, the system would also be ready to be applied to the other handlebar if desired by the team since all other components are ready at the workshop.

#### References

1. Australian Bureau of Statistics, 7501.0 - Value of principal agricultural commodities produced, Australia, Preliminary, 2016-17, 2018. Available at: <https://www.abs.gov.au/Ausstats/abs@.nsf/0/4AC458DB13299EF1CA2573EC0073A449?OpenDocument>.

2. Agriculture: A \$2.4 Trillion industry worth protecting, 2015. Available at: <https://croplife.org/news/agriculture-a-2-4-trillion-industry-worth-protecting/>.
3. Petit S., et al. 2015. "Ecological intensification through pesticide reduction: weed control, weed biodiversity and sustainability in arable farming". *Environ. Manage.* 56: 1078-1090.
4. Abouzienna H.F., W.M. Haggag. 2016. "Weed control in clean agriculture: a review". *Planta Daninha* 34(2): 377-392.
5. Baumann P.A., P.A. Dotray, E.P. Prostko. 2008. "Herbicides: how they work and the symptoms they cause". P. 1-12. Available at: <https://agriflifeextension.tamu.edu/library/gardening/herbicides-how-they-work-and-the-symptoms-they-cause/>.
6. Appleby A.P. 2005. "A history of weed control in the United States and Canada-a sequel". *Weed Sci.* 53(6): 762-768.
7. Khan M.H., N. Khan, N. Badshah. 2003. "Effect of weedicides and hand weedings on the yeild of onion (*Alliam cepa* L.)". *Asian J. Plant Sci.* 2(6): 464-466.
8. Tu M., C. Hurd, J.M. Randall. 2001. „Weed control methods handbook: tools & techniques for use in natural areas". The Nature Conservancy. Available at: <http://tncweeds.ucdavis.edu>.
9. Varshney S., S. Hayat, M.N. Alyemini, A. Ahmad. 2012. "Effects of herbicide applications in wheat fields: Is phytohormones application a remedy?" *Plant Signal. Behav.* 7(5): 570-575.
10. Debenest T., J. Silvestre, M. Coste, E. Pinelli. 2010. "Effects of pesticides on freshwater diatoms". *Rev. Environ. Contam. Toxicol.* 203: 87-103.
11. Yamaha Motor Australia. „Grizzly 700". 2017. Available at: <https://www.yamahamotor.com.au/products/motorcycle/atvrov/utility-atv/grizzly-700>.
12. Ouye J. *Weighted criteria matrix*. Facility Technics Facility Management Consulting, 505 17th Street, Suite 300, Oakland, CA 94612.
13. Gonzalez-de-Santos P., et al. 2017. „Fleets of robots for environmentally-safe pest control in agriculture". *Precision Agriculture* 18: 574-614.
14. Massy-Westropp N.M., T.K. Gill, A.W. Taylor, R.W. Bohannon, C.L. Hill, 2011. "Hand grip strength: age and gender stratified normative data in a population-based study". *BMC Res. Notes* 4: 127.
15. Shrivastava D. 2014. "Designing of All Terrain Vehicle (ATV)". *Int. J. Sci. Res. Publ.* 4(12).
16. Raagul Srinivasan K.A., J. Jawagar Shrehari. 2006. "Design, analysis and fabrication of allterrain vehicle (Quad-Bike)". *Int. J. Inn. Res. Sci. Eng. Tech.* 5(11): 12-26.
17. Bashash S., K. Vora, N. Jalili. 2010. "Distributed-parameters modeling and control of rod-type solid-state actuators". *J. Vib. Control* 17(6): 813-825.
18. AZO Materials, AISI 1018 Mild/Low Carbon Steel. 2012. Available at: <https://www.azom.com/article.aspx?ArticleID=6115>.
19. What is an H-Bridge? H-Bridge concept. 2018. Available at: <https://www.build-electronic-circuits.com/h-bridge/>.



Scientific Journal of Silesian University of Technology. Series Transport is licensed under a Creative Commons Attribution 4.0 International License